The processing of double-strand breaks and binding of single-strand-binding proteins RPA and Rad51 modulate the formation of ATR-kinase foci in yeast

Karine Dubrana*, Haico van Attikum‡, Florence Hediger§ and Susan M. Gasser¶

Friedrich Miescher Institute for Biomedical Research, Maulbeerstrasse 66, CH-4058 Basel, Switzerland

*Present address: Commissariat à l'Energie Atomique, IRCM, Laboratory of Radiobiology and Oncology, 92265 Fontenay aux Roses, France
‡Present address: Leiden University Medical Center, Department of Toxicogenetics, Einthovenweg 20, 2300 RC Leiden, The Netherlands
§Present address: Dr F. Vonmoos-Hediger, Philip Morris International, Toxicological Product Assessment, Quai Jeanrenaud 56, 2000 Neuchâtel, Switzerland
¶Author for correspondence (e-mail: susan.gasser@fmi.ch)

Accepted 20 September 2007
Journal of Cell Science 120, 4209-4220 Published by The Company of Biologists 2007
doi:10.1242/jcs.018366

Summary

Double-strand breaks (DSB) in yeast lead to the formation of repair foci and induce a checkpoint response that requires both the ATR-related kinase Mec1 and its target, Rad53. By combining high-resolution confocal microscopy and chromatin-immunoprecipitation assays, we analysed the genetic requirements for and the kinetics of Mec1 recruitment to an irreparable HO-endonuclease-induced DSB. Coincident with the formation of a 3′ overhang, the Mec1-Ddc2 (Lcd1) complex is recruited into a single focus that colocalises with the DSB site and precipitates with single-strand DNA (ssDNA). The absence of Rad24 impaired cut-site resection, Mec1 recruitment and focus formation, whereas, in the absence of yKu70, both ssDNA accumulation and Mec1 recruitment was accelerated. By contrast, mutation of the N-terminus of the large RPA subunit blocked Mec1 focus formation without affecting DSB processing, arguing for a direct involvement of RPA in Mec1-Ddc2 recruitment. Conversely, loss of Rad51 enhanced Mec1 focus formation independently of ssDNA formation, suggesting that Rad51 might compete for the interaction of RPA with Mec1-Ddc2. In all cases, Mec1 focus formation correlated with checkpoint activation. These observations led to a model that links end-processing and competition between different ssDNA-binding factors with Mec1-Ddc2 focus formation and checkpoint activation.

Supplementary material available online at
http://jcs.biologists.org/cgi/content/full/120/23/4209/DC1

Key words: Double-strand break, ATR-related kinase, Checkpoint, Single-stranded DNA, Rad24, RPA, Rad51

Introduction

An unrepaired double-strand break (DSB) in chromosomal DNA can lead to a potentially dangerous loss of heterozygosity or to chromosomal rearrangements through translocation or recombination events. DSBs are often induced by ionising radiation or chemical insult, yet can arise during an unperturbed cell cycle, particularly during DNA replication (Nyberg et al., 2002). In haploid budding yeast, the persistence of a single broken chromosome leads to a cell cycle arrest in G2 via activation of a Rad9/Rad53-dependent checkpoint response (Melo and Toczyski, 2002). Similar damage-induced checkpoint pathways function in higher eukaryotes and their activation not only ensures cell cycle arrest, but also promotes repair. Not surprisingly, there is a strong correlation between heritable mutations in these pathways and increased rates of human cancer (Shiloh, 2003).

In most species, activation of the DNA-damage-checkpoint response involves one or more members of the PI3 kinase family, including the DNA-dependent protein kinase catalytic subunit (DNA-PKcs), the ataxia telangiectasia mutated (ATM) and the ATM-related (ATR) kinase. In budding yeast, ATM and ATR are encoded by *TEL1* and *MEC1*, respectively, and there is no DNA-PK. Although it is still unclear precisely how DNA-PKcs, ATM and ATR are induced and regulated, in all cases the recruitment to sites of damage is a crucial activation step that is generally facilitated by specific binding partners. For instance, DNA-PKcs requires the yKu70-yKu80 heterodimer for recruitment to DSBs, whereas ATM requires Nbs1 of the MRN complex (Falck et al., 2005). The localisation of ATR at sites of DNA damage requires its partner ATRIP, which has been proposed to associate with replication protein A (RPA)-coated ssDNA (Rouse and Jackson, 2002; Zou and Elledge, 2003). RPA-bound ssDNA accumulates at stalled replication forks and is generated by end-resection at other types of lesions (Adams et al., 2006; Jazayeri et al., 2006). After recruitment to sites of DNA damage, PI3 kinases then differentially phosphorylate a number of substrates, including Chk1 and Chk2, to induce cell cycle arrest and facilitate DNA repair (Jeggo et al., 1998; Wright et al., 1998).

In budding yeast, the ATR-related kinase Mec1 plays a central role in the DNA-damage response, whereas the role of Tel1 is more minor (Sanchez et al., 1996; Mantiero et al., 2007). All DNA-damage-checkpoint functions that depend on Mec1 kinase activity also require the ATRIP-related cofactor Ddc2 (Lcd1) (Paciotti et al., 2000; Rouse and Jackson, 2000). Like ATRIP, Ddc2 binds both double-stranded (ds)- and ssDNA in vitro, and can interact with an RPA-coated ssDNA substrate (Rouse and Jackson, 2002; Zou and Elledge, 2003).

Although mutation of the Mec1 C-terminus impairs its association with RPA, the Mec1-RPA interaction requires the presence of Ddc2 even in a two-hybrid assay, suggesting the existence of a tripartite binding interface between Mec1-Ddc2 and RPA (Nakada et al., 2005).

In yeast, the endonuclease Mre11-Rad50-Xrs2 (MRX complex) and the exonuclease Exo1 are needed to generate ssDNA at a DSB. The MRX complex recruits Tel1, although loss of Tel1 itself has only minor effects on end-processing (Mantiero et al., 2007). Once nucleases convert the break to an RPA-coated 3′ overhang, Mec1-Ddc2 recruitment and the subsequent phosphorylation of Rad53 lead to a checkpoint response that triggers cell cycle arrest. Although the checkpoint activation that arises from a unique unrepaired DSB depends almost exclusively on Mec1-Ddc2, it was shown that the MRX-Tel1 interaction is sufficient to stimulate the downstream response in the presence of multiple lesions (Mantiero et al., 2007), a situation reminiscent of the response to γ-irradiation observed in mammalian cells.

Using GFP-tagged fusion proteins, it has been shown that some checkpoint proteins and DNA-repair factors accumulate in subnuclear foci upon the induction of DNA damage; notably, Ddc2 foci were observed by 30 minutes and up to 24 hours post-DSB induction (Lisby et al., 2004; Melo et al., 2001). The cytology of Mec1, by contrast, has not been monitored, even though chromatin immunoprecipitation (ChIP) assays have shown that Mec1 associates with subtelomeric damage and DNA breaks (Kondo et al., 2001; Rouse and Jackson, 2000). The absence of a kinetic analysis of Mec1-Ddc2 binding led us to examine generally the signals that recruit Mec1 to a unique DSB. Here, we correlate this event to the appearance of ssDNA at the DSB and show that it is upstream of DNA-damage-checkpoint activation.

We found that a fully functional Myc-tagged Mec1 protein accumulates during 1-4 hours after the induction of a DSB in a single focus that coincides with the HO-cleaved *MATalpha* locus. Although the association of Mec1 with DNA was Ddc2-dependent, it did not require the kinase activities of either Mec1 or Rad53. A quantitative PCR analysis of the DNA immunoprecipitated with Mec1 revealed a specific enrichment for ssDNA particularly at early time points. The comparative kinetics of Mec1 recruitment in mutants suggests that the recruitment of Mec1-Ddc2 at high levels requires the creation of a 3′ overhang. Surprisingly, however, we found that Mec1 focus formation and checkpoint activation were impaired in a strain bearing a point mutation in the OB-fold domain 1 of Rfa1 (*rfa1*-t11), even though end resection was normal. This implicates Rfa1 directly in Mec1-Ddc2 recruitment, consistent with interactions documented by two-hybrid studies (Nakada et al., 2005). In cells lacking the strand-exchange factor Rad51, Mec1 foci form even more readily, although strand processing is slightly impaired. This suggests that Rad51 might compete for Mec1 association with RPA at a processed DSB. This would provide a means to forestall checkpoint activation when repair occurs efficiently either by non-homologous end-joining (NHEJ) or by homologous recombination (HR) using a sister chromatid. Indeed, we found that that the low level of foci formed in the presence of homologous donor sequences were resolved when HR could take place. These observations led to a model that links end-processing and competition between different ssDNA-binding factors with Mec1-Ddc2 focus formation and checkpoint activation.

Results

Mec1 forms a large single focus at an induced DSB

To analyse the cytology of Mec1 during the DNA-damage response in backgrounds that impair DNA repair and checkpoint activation, we used a well-characterised system in budding yeast that allows the induction of a DSB at the *MATalpha* locus by galactose-induced expression of the yeast HO endonuclease (Fig. 1A). Recombination-mediated repair is suppressed because of deletion of the homologous-mating-type loci, *HMR* and *HML*, and, although the NHEJ pathway is functional in these cells, continuous HO expression allows re-cleavage and persistence of the break (Lee et al., 1998). By tagging Mec1 with a Myc epitope, we were able to follow its behaviour on a single-cell level by immunostaining. In the absence of DNA damage, Myc-Mec1 had a dispersed but slightly punctate localisation within the yeast nucleoplasm (0 hours, Fig. 1B). These weak Mec1 speckles did not colocalise significantly with telomeres (see Mec1-Sir4 double staining, Fig. 2A) or with Orc2 (data not shown). Following induction of the DSB on galactose, nuclear Mec1 accumulated in a single bright focus (Fig. 1B). By 4 hours after DSB induction, the focus was found in nearly all cells (note that only equatorial confocal sections representing roughly 70% of the nuclear volume were scored). Without cleavage, a Mec1 focus formed in roughly 1% of cells, probably reflecting an incomplete repression of HO or else spontaneous damage (Lisby et al., 2004). Although cell growth continued after DSB induction, there was no significant change in Mec1 protein levels in response to the break (data not shown). Under the conditions used for induction of the endonuclease, 4 hours is the time required to complete a cell cycle, activate the Rad53 kinase and accumulate G2-phase cells (for Rad53 activation, see below). Therefore, we concentrated our analysis on events in this time period.

To prove that the Mec1 focus coincides with the DSB, we inserted an array of *lacO* repeats 4.4 kb from the HO consensus and coupled Mec1 staining with direct epifluorescence of lacI-GFP. By 4 hours on galactose, 70% of the Mec1 staining (Fig. 1B, red, bottom-right panel) accumulated within a radius of 0.4 μm from the centre of the *MAT*-lacI fluorescence (Fig. 1B, green), indicating colocalisation. To correlate the kinetics of Mec1 focus formation with the ability of Mec1 to bind the cut site, we performed ChIP for Myc-Mec1 and multiplex PCR with multiple probes from the *MAT* locus (primer positions in Fig. 1A; PCR data in supplementary material Fig. S1). By 1 hour on galactose, we detected a ninefold enrichment for Myc-Mec1 at HO2 (+0.6kb from the DSB) over the background at an uncleaved control site (*SMC2*, Fig. 1C). This increased to 40- and 52-fold by 2 hours and 4 hours of HO induction, respectively. This massive enrichment was specific for Myc-Mec1; beads coated with anti-HA yielded significantly lower background signals (Fig. 1C), as did untagged strains with anti-Myc-coated beads (data not shown). Recruitment was slightly less-efficient at sites 2 kb or 3 kb away (HO1 and HO3, respectively), and the hierarchy of enrichment (HO2>HO1>HO3) argues that Mec1 spreads from the cut site. This is further supported by the fact that we detected Mec1-spreading up to 9.6 kb from the HO cut site by 4 hours after

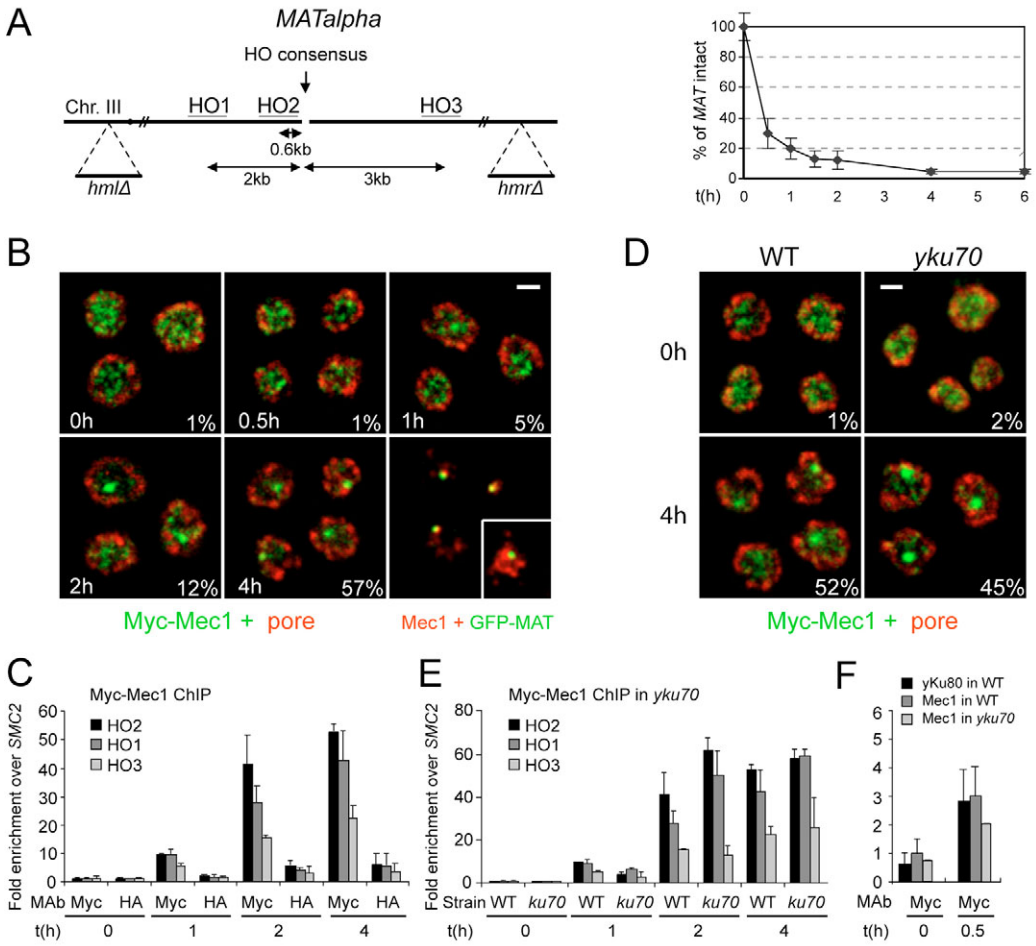

Fig. 1. Mec1 recruitment to the HO-endonuclease-induced DSB leads to the formation of large foci in most cells. (A) Crucial features of the yeast test strain JKM179 are shown. This strain lacks HM loci on chromosome 3 and contains an integrated galactose-inducible HO endonuclease gene. PCR fragments used to analyse ChIP experiments are labelled HO1, HO2 and HO3. (Graph) The efficiency of cleavage was quantified by PCR across the HO cleavage site, normalised to *t*=0 and plotted against time (hours after addition of 2% galactose). (B) The JKM179 strain was modified by an N-terminal Myc-epitope fusion to the genomic *MEC1* gene, producing GA1529. Cells were prepared for IF after 2 hours of growth on glucose (0-hour time point) or after 0.5, 1, 2 or 4 hours on galactose. IF with anti-Myc (9E10 Mab, green) and anti-nuclear-pore (Mab414, red) was imaged on a Zeiss LSM510 confocal microscope. Single equatorial focal sections are shown. Only 70% of the nuclear volume is imaged and the percentage of such sections with a single bright Mec1 focus is indicated. In the lower right-hand panel, Myc-Mec1 (red) is visualised at 0 (inset) and 4 hours on galactose in a strain that carries a *lacO* array inserted 4.4 kb from the HO cut site and a *GFP-lacI* fusion (green). (C) ChIP for Myc-Mec1 at the indicated time points after induction of GAL::HO endonuclease on galactose. The 0-hour time point represents cells exposed to glucose for 2 hours to repress HO expression. Anti-Myc (9E10) and anti-HA (12CA5) were used for ChIP. DNA purified from input, the Myc-Mec1 (Myc) or HA (HA) IPs were analysed by multiplex PCR primers for the three HO sites shown in A and for the uncleaved *SMC2* gene (see supplementary material Fig. S1). Quantitation of the products is presented as the ratio of the HO1, HO2 or HO3 signals to *SMC2* in the IP, normalised to the same ratio in the corresponding input. In this way, changes in relative abundance of primer sites due to end-resection are factored out of the enrichment value. (D) Myc-Mec1 localisation as described in B in a derivative of JKM179 that lacks yKu70 (GA-1796). (E) Myc-Mec1 binding was analysed by ChIP as described in D using JKM179 (wild type, WT) and a derivative deleted for the gene encoding yKu70 (GA-1796). (F) Myc-Mec1 and yKu80-Myc binding was analysed by ChIP as described in C, but after 30 minutes on galactose in the JKM179 strain (WT, black and dark-grey bars) and in a derivative deleted for *yku70* (light-grey bars). Bars, 1 μm.

break induction (supplementary material Fig. S2). We conclude that Mec1 accumulates to very high levels at a DSB, and that this correlates with focus formation in most cells.

Mec1 binds rapidly at low levels to DSBs independently of yKu

In mammalian cells, the Ku70-Ku80 heterodimer helps recruit the kinase DNA-PKcs to DNA ends (Falck et al., 2005). In yeast, we have shown a significant enrichment of yKu at an induced DSB by 30 minutes after HO induction (Martin et al., 1999). To see whether yKu regulates Mec1 recruitment to the HO cut site, we monitored the Mec1 accumulation at *MAT* by immunofluorescence (IF) and ChIP in a strain bearing a *yku70* deletion, which also eliminates yKu80 binding to DNA ends (Martin et al., 1999; Frank-Vaillant and Marcand, 2002). Quantitation of the Myc-Mec1 foci in *yku70* showed that 45% of the cells have Myc-Mec1 foci at 4 hours of induced cleavage (Fig. 1D). ChIP analysis confirmed that Mec1 is efficiently

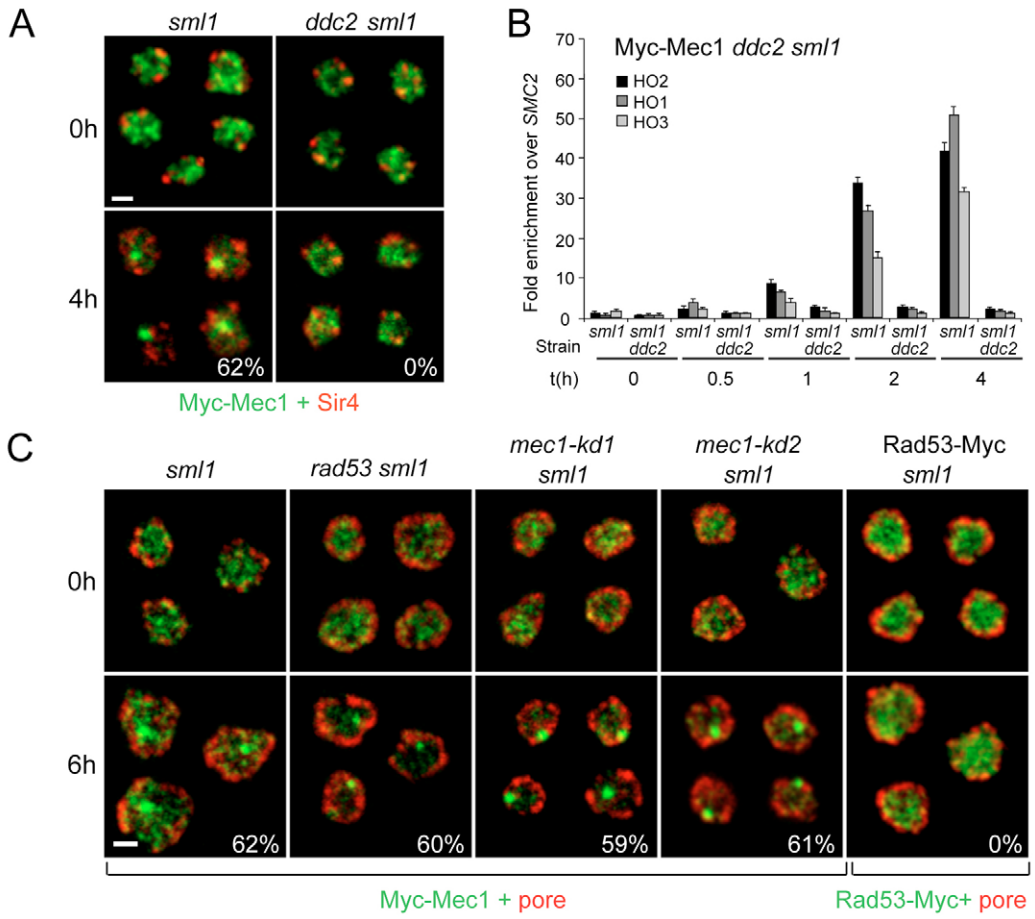

Fig. 2. Mec1 focus formation requires Ddc2, but not Mec1 or Rad53, kinase activity. (A) Myc-Mec1 localisation after HO induction for 0 and 4 hours in JKM179 derivatives deleted for both *ddc2* and *sml1* (GA1825) or for *sml1* alone (GA1817). IF was performed with anti-Myc (9E10; green) and with affinity-purified anti-Sir4 (red) antibodies. Values correspond to the percentage of nuclei exhibiting a single bright Mec1 focus above a low background of diffuse Mec1. (B) Myc-Mec1 ChIP assay was performed as described in Fig. 1D using JKM179 derivatives carrying deletions for *ddc2 sml1* or *sml1* alone. (C) Myc-Mec1 localisation in JKM179-derived strains carrying deletions for *sml1*, for *sml1* and *rad53* together, or for *sml1* with *Myc-mec1-kd1* or *Myc-mec1-kd2* mutations. IF for Myc-Mec1 (green, 9E10) and anti-pore (red, Mab414) is shown and the percentage of nuclei with one bright Mec1 focus is given. To the right, a JKM179 derivative expressing Myc-Rad53 was analysed by anti-Myc IF (green) after cut induction. Bars, 1 μm.

recruited (Fig. 1E). To see whether the early recruitment of Mec1-Myc might be yKu dependent, we compared the timing and dependence of Mec1-Myc at an early time point after HO induction. At 30 minutes on galactose, yKu and Mec1 had very similar recruitment levels (threefold over background, Fig. 1F). In the *yku* mutant, the recruitment of Mec1 was not significantly changed (Fig. 1F). Thus, both yKu and Mec1-Ddc2 are rapidly recruited to a low level in an apparently independent fashion. However, by 2 hours of induction, the Mec1 signal at 2 kb from the HO site (HO1) was 1.5-fold higher in *yku70* cells than in the wild-type control (Fig. 1E). This correlates with an enhanced rate of 3′-overhang formation in *yku* mutants, because the rate at which cleavage occurs and processing is initiated do not vary in these strains (Frank-Vaillant and Marcand, 2002; Lee et al., 1998). Our observation suggests an involvement of ssDNA formation in Mec1 recruitment.

Ddc2 is required for Mec1 focus formation

If the formation of Mec1 foci reflects the physiological association of Mec1 with processed DNA, then focus formation should be dependent on Ddc2. To analyse this, we scored for Mec1 focus formation in a *ddc2* mutant. Because Ddc2 is essential for viability, its deletion must be coupled with the *sml1* deletion to restore dNTP levels and suppress lethality (Zhao et al., 1998).

When the DSB is induced in the absence of Ddc2, we observed that Myc-Mec1 remained diffuse throughout the nucleus, whereas it formed distinct foci both in wild-type and *sml1* strains (Fig. 1B, Fig. 2C). We combined the Mec1 staining with labelling of Sir4 to confirm that the checkpoint response was compromised by the *ddc2* mutation. Indeed, Sir4 remained in perinuclear foci 4 hours after induction of the DSB, rather than becoming partially dispersed (Fig. 2A) (Martin et al., 1999).

We confirmed by ChIP for Myc-Mec1 that Mec1 fails to associate with the HO cut in the absence of functional Ddc2 (Fig. 2B), whereas, in the *sml1* control, Mec1 recruitment was the same as in wild-type cells (Fig. 2C). We conclude that the absence of Ddc2 not only impairs checkpoint response but abolishes Myc-Mec1 binding at the cleaved and processed

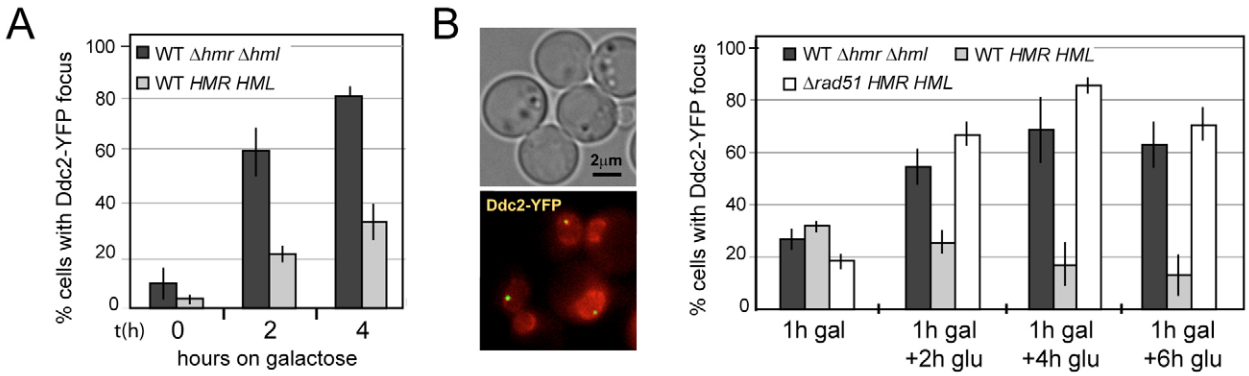

Fig. 3. Ddc2-YFP foci disappear rapidly upon repair when donor loci are present for HR. (A) Ddc2-YFP fusion allows visualisation of the same Mec1-Ddc2 foci detected by IF after DSB induction (see Figs 1 and 2). We monitored the presence of Ddc2-YFP foci in two isogenic strains either bearing wild-type (WT) HML and HMR donor loci (KD-131; light-grey bars) or bearing *hml* and *hmr* deletions (GA-2358; dark-grey bars) after induction of the HO endonuclease on galactose for the indicated times. (B) Focus disappearance requires donor loci and Rad51. To show whether loss of foci coincides with repair by HR, we scored for Ddc2-YFP foci both in the strains used in panel A and in KD-132, in which wild-type HML and HMR are combined with a full *rad51* deletion. Cells were grown on YPLGg overnight and *GAL::HO* was induced by 2% galactose for 1 hour. Thereafter, glucose was added to repress the endonuclease. The fluorescence image (bottom) shows a panel of typical cells bearing Ddc2-YFP (yellow) on a background of Nup49-CFP signal (red) after 1 hour of growth on galactose with 2 hours of glucose recovery. The corresponding phase image is also shown (top). (Graph) The percentage of cells with Ddc2-YFP foci were monitored in all strains after 1 hour of growth on galactose (gal), and then again after 2, 4 and 6 hours on glucose (glu). Note that the processing of DSBs continues even after the switch to glucose. Bar, 2 μm.

MATalpha locus, eliminating focus formation. These results confirm cytologically the interdependence between Mec1 and Ddc2, which was deduced from ChIP and two-hybrid data (Nakada et al., 2005; Rouse and Jackson, 2002). Because Ddc2 is required for the downstream checkpoint response, these results also suggest that the checkpoint response could be promoted by Mec1 focus formation (see below).

Checkpoint kinase activation is not required for Mec1 binding to DSB

We next examined whether Mec1 focus formation could require Mec1 or Rad53 kinase activities. Previous ChIP studies have shown that mutations in Mec1 that abolish kinase activity do not abolish the initial association of the kinase with an HO-induced DSB (Nakada et al., 2005). However, it was not clear whether such mutations would affect Mec1 focus formation, which results from a continued accumulation of Mec1-Ddc2 at the processed break. To test this, we scored Mec1 focus formation in strains carrying point mutations that eliminate Mec1 kinase activity (Paciotti et al., 2001) or in a strain lacking Rad53 kinase. In both cases, the mutations were coupled with a *sml1* deletion, which alone does not impair the checkpoint response or Mec1 focus formation (Fig. 2C) (Zhao et al., 1998). We observed that the efficiency of Myc-Mec1 focus formation was unaffected by the absence of either Mec1 kinase activity (*Myc-mec1*-kd1 and *Myc-mec1*-kd2) or the downstream kinase Rad53 (Fig. 2C). Quantitation of foci at 2-hour and 4-hour time points confirmed that the kinetics of focus formation were also unchanged (data not shown). We further examined whether Rad53-Myc itself forms foci in the presence of a DSB, yet, unlike that observed for Mec1, we detected no accumulation of Rad53 at the cut site (Fig. 2C). Although we assume that Rad53 must bind near the DSB, this result suggests that it associates transiently without accumulating in the repair focus. Finally, we scored Mec1 focus formation in a strain lacking the ATM homologue Tel1. We monitored no requirement for Tel1 kinase activity for Mec1 focus formation (supplementary material Fig. S3), consistent with results showing that Tel1 is dispensable for the Mec1-mediated checkpoint response. This is not true in mammalian cells, in which ATM appears to contribute to ATR recruitment at DSBs (Adams et al., 2006).

Our results indicate that the Mec1-mediated phosphorylation of target proteins at DSBs, including RPA and other repair factors, is not needed for the massive accumulation of Mec1 into a focus at the DSB. Modification of these factors might nonetheless contribute to either a repair pathway or else to checkpoint activation.

Mec1-Ddc2 focus formation is reversible upon repair by homologous recombination

To better understand the nature of the Mec1-Ddc2 foci that we observed, we examined whether foci would form under conditions that allow efficient DSB repair by HR. In wild-type (WT) yeast cells that carried intact *HMR* and *HML* loci, the break that was induced at *MATalpha* was repaired by gene conversion with one of these homologous loci. We first examined the accumulation of Ddc2-YFP foci under continuous GAL::HO induction, by scoring foci after 0, 2 and 4 hours of growth on galactose (Fig. 3A). The increase in Ddc2-YFP foci in a strain lacking *hmr* and *hml* agrees well with frequency of Myc-Mec1 foci scored by IF (Fig. 1). In strains bearing donor sequences for recombination (WT, *HML HMR*), the values were much lower, but foci still appeared, probably because of the continuous expression of the HO endonuclease, which then re-cuts the *MAT* locus after repair is achieved. To eliminate this re-cleavage and allow repair, we shut off the HO endonuclease after 1 hour on galactose by adding glucose. In Fig. 3B, we show that the Ddc2-YFP foci that form after 1 hour on galactose are reversible, yet only when repair by HR is possible. In strains in which the *hmr* and *hml* donor sequences were deleted, or that were deleted for

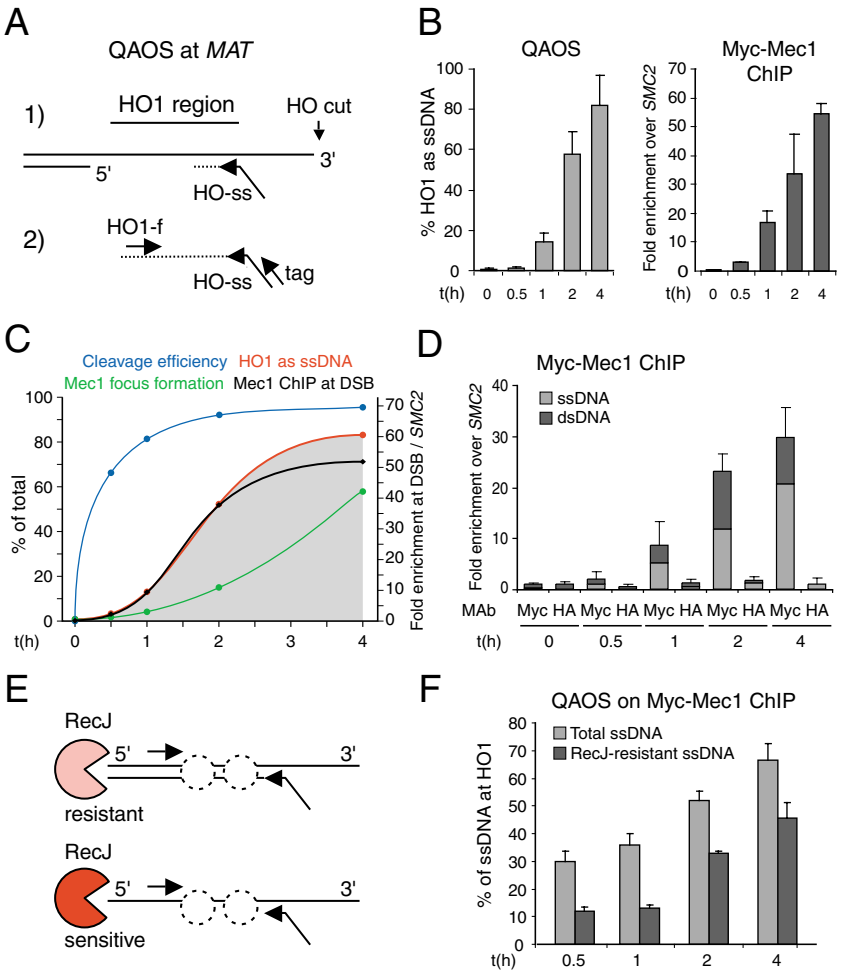

Fig. 4. ssDNA is enriched in Myc-Mec1 precipitates. (A) Schematic for QAOS (Booth et al., 2001) near the HO cleavage site of *MATalpha* is shown. (B, left) The percentage of HO1 signal that exists as ssDNA was measured by QAOS in the input DNA at the indicated time points after HO cut induction. (Right) Myc-Mec1 ChIP was performed in JKM179 after galactose induction of the HO endonuclease. Fold enrichment of Mec1 over SMC2 at the HO2 site (0.6 kb away from the HO cleavage site) is shown. (C) The efficiency of HO cut-site cleavage (Fig. 1A, shown here in blue) is plotted against the percentage of ssDNA at HO1 in input DNA (Fig. 2B, red), the percentage of cells showing a single bright Mec1 focus (Fig. 1B, green) and the fold enrichment of Myc-Mec1 at the DSB over SMC2 (Fig. 1C, HO2, black). (D) Myc-Mec1 ChIP was performed after galactose induction of the HO endonuclease as in Fig. 1C. The IP DNA was then subjected to QAOS to quantify the fraction of the precipitated HO1 site that is ssDNA. The amount of ssDNA (light grey) is plotted as a fraction of the total Myc-Mec1-bound DNA. (E) Schematic of the degradation of Myc-Mec1-bound DNA by the RecJ exonuclease. RecJ is a 5′-to-3′ exonuclease that degrades only ssDNA. It will not degrade DNA that is ds at the 5′ end. (F) The amount of ssDNA at HO1 was measured by QAOS on Myc-Mec1-bound DNA at the indicated time points after HO induction either before or after incubation with RecJ endonuclease for 3 hours at 37°C, but after removal of proteins by proteolysis and phenol extraction.

rad51 such that no repair by recombination was possible, the Ddc2-YFP foci continued to accumulate for 4-6 hours (Fig. 3B). We conclude that, when rapid repair is possible, Mec1-Ddc2 foci might form transiently, but do not persist. This is consistent with the observation that, under conditions that allow mating-type switching in yeast, a checkpoint response is not provoked by HO cut induction at the *MAT* locus and its repair by a gene conversion event with either *HML* or *HMR* sequences (Pellicioli et al., 2001). It appears that repair by HR prevents extensive end-resection and, in turn, Mec1-Ddc2 focus formation.

Mec1-bound chromatin is enriched for ssDNA

We have shown above that checkpoint kinases and yKu are not needed to recruit Mec1-Ddc2 to a DSB. What, then, is the signal that allows a massive accumulation of Mec1-Ddc2 at a DSB? Studies in yeast and mammalian cells have suggested that a nuclease activity is needed to process the DSB and to create an RPA-coated ssDNA fibre that can recruit Mec1-Ddc2 (Adams et al., 2006; Jazayeri et al., 2006; Nakada et al., 2004; Zou and Elledge, 2003). However, recovery of Mec1-Ddc2 bound to ssDNA at a DSB in vivo has not been demonstrated.

To test the relationship between Mec1 accumulation at the break and creation of the 3′ single-strand overhang, we first examined whether the kinetics of 5′-to-3′ degradation at the induced DSB correlated with the binding of Mec1. We monitored ssDNA formation with a quantitative amplification procedure called QAOS (quantitative amplification of ssDNA) (Booth et al., 2001). QAOS is a real-time PCR assay based on an initial round of DNA synthesis at low temperature with a bimodal primer that has ~20 nucleotides of homology with the region of interest fused to a non-related sequence. In a second step, quantitative real-time PCR is performed at stringent temperatures using another set of primers that quantifies the amount of single-strand template that was present in the initial synthesis step (Fig. 4A). The zero and the 100% baselines were established by using a fully dsDNA or a fully denatured template. We found that the amount of ssDNA at a site 2 kb from the HO cleavage site (HO1) in the total DNA ranged from 0.8% in the absence of galactose to over 80% after 4 hours of induction (Fig. 4B, light-grey bars), correlating with the kinetics of Mec1 recruitment to the DSB determined by ChIP (Fig. 4B, dark-grey bars). If we plot the kinetics of Mec1 focus formation, ssDNA accumulation and Mec1 recruitment as monitored by ChIP, we see that the appearance of ssDNA correlates precisely with Myc-Mec1 recruitment, and not with formation of the cut. Mec1 focus appearance, by contrast, lags behind (Fig. 4C).

To test whether the ssDNA that accumulates at the cut site is bound to Mec1, we quantified the amount of ssDNA recovered in the Mec1-Myc ChIP. The specificity of the QAOS assay for ssDNA was confirmed by treating the Mec1-

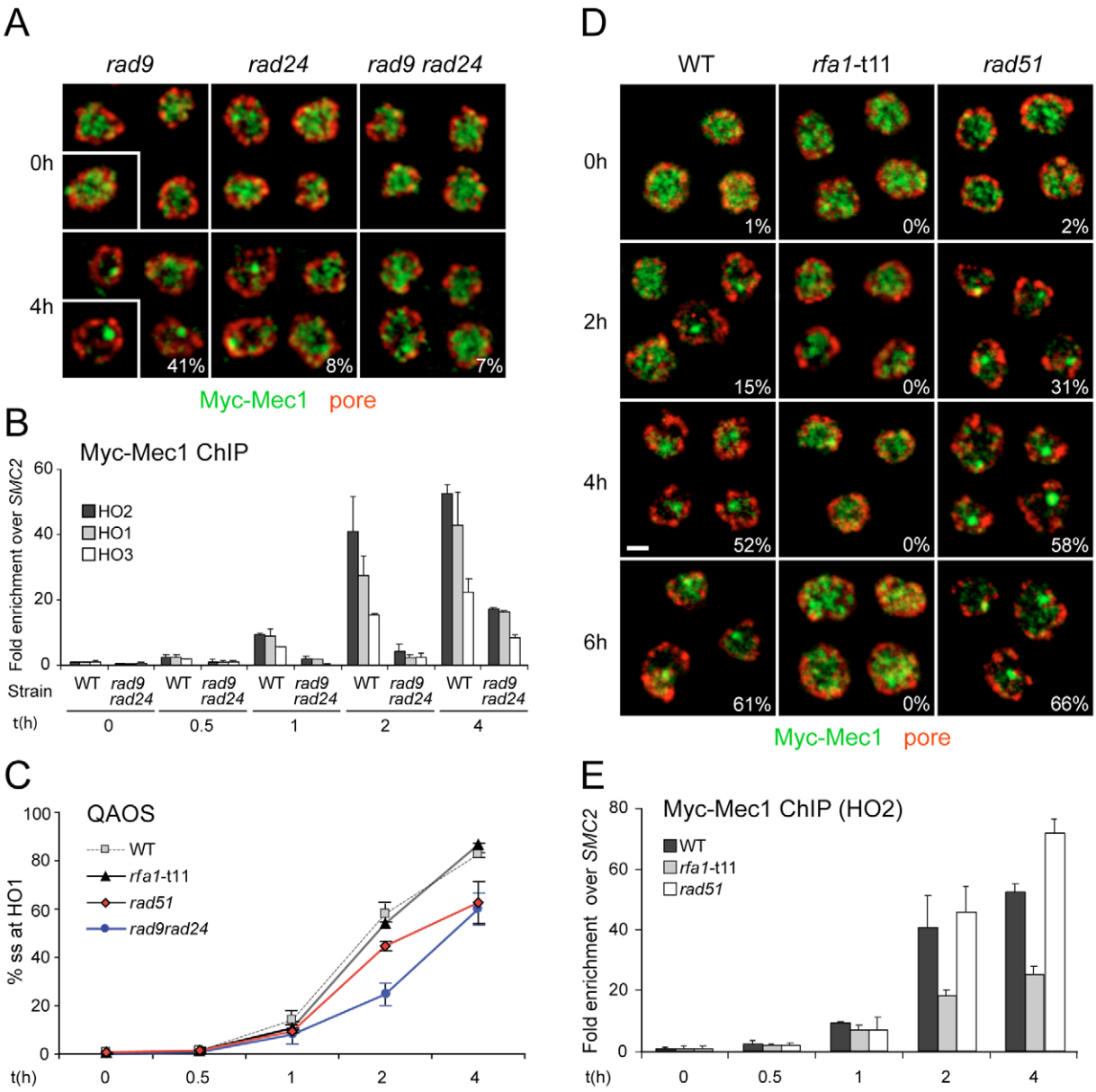

Fig. 5. Myc-Mec1 focus formation and recruitment in *rad24*, *rfa1*-t11 and *rad51* mutants. (A) Myc-Mec1 localisation was determined by IF in JKM179 derivatives expressing Myc-tagged Mec1 (GA1529, shown in the insets in the *rad9* panels), or in strains deleted for *rad9*, for *rad24* or both, after 0 and 4 hours of HO induction on galactose. IF was conducted as in Fig. 1B. Values correspond to the percentage of nuclei exhibiting a single Mec1 focus. (B) Myc-Mec1 ChIP at the HO cleavage site as described in Fig. 1C using the *rad9 rad24* double-deletion strain or the wild-type (WT) JKM179 derivative. (C) The percentage of ssDNA at the HO1 site was measured, after HO induction, by QAOS on total DNA from the JKM179-derivative GA1529 (WT), or from JKM179 with null alleles of *rad51*, *rad9 rad24* or *rfa1*-t11. (D) IF as in Fig. 1B on the wild-type JKM179 derivative (GA1529) and isogenic strains bearing *rfa1*-t11 (GA2158) or a *rad51* deletion (GA2163). Values correspond to the percentage of nuclei exhibiting a single bright Mec1 focus above the background of diffuse Mec1. Note that absence of a focus does not necessarily mean that no Mec1-Ddc2 binds the DSB but rather that the level is below the threshold of detection by IF. (E) Myc-Mec1 ChIP as described in Fig. 1C on JKM179 carrying either the *rfa1*-t11 mutation or a *rad51* deletion. Results are shown for the HO2 probe only, although all probes showed analogous results. Bar, 1 μm.

chromatin-immunoprecipitated DNA with Mung-bean nuclease prior to amplification, which eliminated the QAOS signal (supplementary material Fig. S4). We then compared the total Mec1-bound DNA with the amount of ssDNA in the precipitated samples at time points following the induction of the DSB (Fig. 4D). All values are presented as enrichment over a non-cleaved site (*SMC2*) to ensure that we monitored only break-specific interactions. We observed that, at all time points, at least half of the HO1 signal recovered with Myc-Mec1 was ssDNA; this increased to 65% at 4 hours (Fig. 4D). Again, the use of a control antibody, anti-HA, confirmed that the precipitation of HO1 DNA is specific to Mec1 (Fig. 4C)

We next studied whether all Mec1-bound DNA is single-stranded. In other words, does Mec1 spread beyond the 3′

overhang, or bind only where resection occurred? To test this, we incorporated a step that would enable the selective degradation of ssDNA bound to Mec1 by a 5′-to-3′ exonuclease (RecJ) (Lovett and Kolodner, 1989). This allowed us to quantify the fraction of Mec1-bound DNA that had dsDNA at its 5′ end, because this would render the bound fragment resistant to RecJ nucleolytic attack (see Fig. 4E). Therefore, following ChIP with Myc-Mec1 at the usual time points after DSB induction, we treated the Mec1-bound DNA with RecJ exonuclease, inactivated the nuclease and then determined what fraction of the Mec1-bound ssDNA was RecJ-sensitive. As shown in Fig. 4F, about 50% of the ssDNA recovered by Mec1 ChIP was sensitive to RecJ. This confirms that much of Mec1 is indeed bound to exclusively ssDNA, and not at the ds-ssDNA junction. By contrast, the fact that roughly half of the ssDNA recovered with Mec1 was resistant to RecJ nuclease (Fig. 4F) most probably reflects Mec1 bound to hybrid ds-ssDNA. Interestingly, at the earlier time points, proportionately less Mec1-bound DNA was dsDNA, suggesting that Mec1 spreads beyond the ssDNA junction into dsDNA at later time points. Interaction of Mec1 with dsDNA is consistent with the fact that Mec1-dependent H2A phosphorylation spreads for 40-50 kb around a DSB before extensive conversion of the surrounding DNA into ssDNA (Shroff et al., 2004). These data are the first direct demonstration that ATR kinase (Mec1) is bound to ssDNA at a processed DSB in vivo (Fig. 4F).

Mec1 recruitment to a DSB is compromised by the absence of Rad24

Because the generation of ssDNA appears to be crucial for Mec1 binding at the unique HO-induced DSB, we investigated whether the kinetics of Mec1 focus formation would be altered by the absence of Rad24, which was shown to suppress the conversion of DNA into ssDNA at DSB and at damaged telomeres (Aylon and Kupiec, 2003; Maringele and Lydall, 2002). In the absence of HO induction, the *rad24* mutant exhibited a diffuse nucleoplasmic pattern of Mec1 staining and, by 4 hours of induction, foci appear in only 8% of the cells (Fig. 5A). At damaged telomeres, the action of Rad24 seems to be counteracted by Rad9 (Lydall and Weinert, 1995; Maringele and Lydall, 2002). We thus analysed Mec1 focus formation in *rad9* and *rad9 rad24* mutants. In the *rad9* mutant, 41% of the cells accumulated bright Myc-Mec1 foci, a value only slightly lower than the 52% observed in wild-type cells (Fig. 5A). Together with the *rad53* data in Fig. 2, this result argues that checkpoint activation is not needed for Mec1 focus formation. Contrary to what was observed at telomeres, the defect in Mec1 focus formation in the *rad24* strain was epistatic to the *rad9* phenotype: notably, the double-mutant phenotype resembled that of the *rad24* single mutant (Fig. 4A).

We next monitored the kinetics of Myc-Mec1 recruitment to the HO cleavage site in wild type and in a *rad9 rad24* double-mutant strain by ChIP. Consistent with the focus-formation data, we observed a striking drop in the efficiency of Mec1 binding near the DSB in the double mutant (tenfold less than wild type at 2 hours and two- to three-fold less at 4 hours; Fig. 5B). The requirement for Rad24 for efficient Mec1 focus formation could either reflect direct contact between Rad24 and Mec1-Ddc2 or could stem from its role in generating the ssDNA template, which in turn would bind RFA and Mec1-Ddc2. We therefore quantified the appearance of ssDNA at the HO1 site by QAOS in the *rad9 rad24* mutant. We found that end-resection in the *rad9 rad24* double mutant was indeed significantly delayed (Fig. 5C). Like the reduction in Mec1 recruitment monitored by ChIP, the effect was most pronounced at 2 hours after HO induction, but persisted until 4 hours. Although this correlation strongly implicates Rad24 in end-resection, and in end-resection in Mec1 recruitment, Rad24 might also contribute to Mec1 recruitment through a second pathway. We note that there was roughly the same level of ssDNA in the *rad9 rad24* mutant at 4 hours as in the wild-type strain at 2 hours, yet Mec1 still bound less efficiently in the double mutant (Fig. 5B,C).

Mec1 recruitment to a DSB is antagonised by *rfa1*-t11 and increased by *rad51* deletion

In vitro studies suggest that RPA and Rad51 compete for ssDNA (Sung, 1997). Because Mec1 recruitment and focus formation correlate with the appearance of ssDNA, we reasoned that these processes might be influenced or regulated by ssDNA-binding proteins, such as RPA or Rad51. To test this, we probed for Myc-Mec1 focus formation in the *rfa1*-t11 mutant and *rad51* deletion strains (Umezu et al., 1998). The *rfa1*-t11 mutant is deficient in strand exchange and recombination functions, yet it supports normal DNA replication and is thus able to bind ssDNA and function with DNA polymerase α (Umezu et al., 1998). Remarkably, in the *rfa1*-t11 mutant, we were unable to detect any Myc-Mec1 focus formation after HO cut induction (Fig. 5D), even when the cleavage reaction continued for 6 hours. We observed that Myc-Mec1 foci formed in 52-61% of wild-type cells by 4 or 6 hours after HO induction, whereas basically no foci were detectable in the *rfa1*-t11 strain.

To confirm the effect of the *rfa1*-t11 mutation on Mec1 binding, we monitored Mec1 recruitment to the DSB by ChIP (Fig. 5E). Although we saw no significant differences before 1 hour of induction, suggesting that the initial low-level recruitment was intact, at the 2- and 4-hour time points Myc-Mec1 recruitment was reduced by half in the *rfa1*-t11 mutant (Fig. 5E). Importantly, this was not due to a lack of resection at the cut site, because the appearance of ssDNA at HO1 in the *rfa1*-t11 mutant occurred at rates comparable to those in the wild-type strain (Fig. 5C). Rather, *rfa1*-t11 appeared to be specifically defective in high-level Mec1 accumulation that leads to focus formation. This suggests that the N-terminus of Rfa1 is directly involved in the accumulation of Mec1-Ddc2 along ssDNA, consistent with the fact that Mec1-Ddc2 bind Rfa1 in an interdependent manner, which reflects direct contact between Mec1 and Rfa1 (Nakada et al., 2005). However, unlike focus formation, Mec1 binding detected by ChIP was not fully abolished in the *rfa1*-t11 mutant. The residual Mec1 binding might be sufficient to stimulate the checkpoint response, albeit with a delay (Fig. 6). It is not surprising that ChIP detected reduced levels of Mec1 that were not scored in the focus assay, because the diffuse background-staining of Myc-Mec1 obscures small Mec1-Ddc2 foci.

Intriguingly, the *rad51* mutant had almost the opposite effect on Mec1 focus formation as the *rfa1*-t11 mutant (Fig. 5D,E). There was a significant increase in Myc-Mec1 foci at early time points (31% vs 15% at 2 hours after induction, Fig. 5D), whereas, at later times, focus-frequency was similar to that

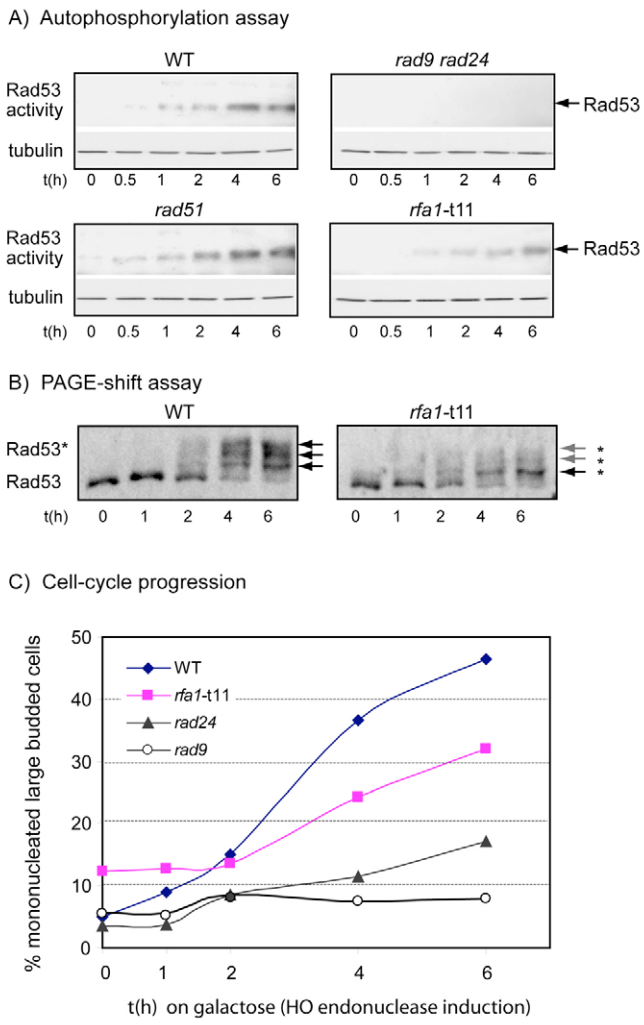

Fig. 6. A functional checkpoint is modulated by rfa1-t11 and Rad51. (A) Rad53 kinase activation was analysed by an in-gel autophosphorylation assay (Pellicioli et al., 1999) at the indicated time points after HO induction. Strains are JKM179 (wild type, WT) or derivatives thereof. Equal loading was scored on the same blot with anti-tubulin (TAT-1). (B) The wild-type and *rfa1*-t11 mutant cells were probed for checkpoint induction by monitoring the shift of phospho-Rad53-Myc (*) by SDS-PAGE. (C) The percentage of mononucleated large budded cells (G2/M arrest) was scored after ethanol fixation and DAPI staining at the indicated time points after HO induction. JKM179 strains and derivatives were used and values represent the mean of three experiments with >300 cells per set.

observed in wild-type cells (61% vs 66% after 6 hours). ChIP data confirmed that Mec1 recruitment occurred efficiently in the absence of Rad51 (Fig. 5E). This is true even though the accumulation of ssDNA was slightly impaired in the *rad51* mutant, at least at 4 hours. Thus, independent of DSB processing, Rfa1 and Rad51 have opposite effects on Mec1 binding at a DSB.

Checkpoint activation is antagonised by *rfa1*-t11 but is increased by *rad51* deletion

To correlate the efficiency of Mec1 recruitment and focus formation with the downstream checkpoint response, we monitored Rad53 activation after HO induction in all these mutants using an in-gel assay for Rad53 autophosphorylation (Pellicioli et al., 1999). This in situ assay is highly sensitive for Rad53 kinase activity; phosphorylation can be accurately quantified by normalising for loading efficiency the immunodetection of tubulin on the same filters (Fig. 6A). We found that the activation of Rad53 kinase was initiated at roughly 1 hour after HO induction in wild-type cells, peaking at 4-6 hours. We observed a slightly more-rapid induction of Rad53 activity in the *rad51* mutant, which correlated positively with the enhanced rate of Mec1 focus formation (Fig. 6A). As expected, there was no checkpoint response whatsoever in the *rad9 rad24* mutant, because Rad9 is an essential cofactor for Rad53 activation. More importantly, however, we noted a reduction in Rad53 activation in the *rfa1*-t11 mutant, which correlated with the reduction in Mec1 recruitment and Mec1 foci formation (Fig. 6A). This is true despite efficient end-resection (Fig. 5D).

Because this delay in checkpoint response allows us to correlate focus formation and high-level Mec1 recruitment with the downstream checkpoint response, we decided to document the effect of the *rfa1*-t11 mutant in two further assays for checkpoint activation. We first made use of a second Rad53 activation assay that monitors the phosphorylation-induced shift in Rad53 mobility. Here, we observed that, whereas wild-type cells showed a dramatic shift in Rad53 migration, the shift was reduced at the same time points in the *rfa1*-t11 mutant (Fig. 6B). To confirm this with another independent assay, we monitored the efficiency with which cells arrest in G2/M as large-budded, mononucleated cells after induction of the DSB, which is a direct measure of the checkpoint arrest. Consistently, we saw that both the *rad24* and *rfa1*-t11 mutations compromise the G2/M arrest such that cells continue through mitosis into the subsequent cell cycle (Fig. 6C). All three assays thus argue that Mec1 recruitment and focus formation correlate with the appearance of ssDNA; both appear to be necessary for proper checkpoint activation in response to a single DSB. All phenotypes are compromised by mutations that impair the processing of the break, whereas *rfa1*-t11 impairs all but end-resection. By contrast, the loss of *rad51* seems to promote focus formation, leading to precocious checkpoint activation, independent of end-resection efficiency.

Discussion

Due to the diversity of lesions induced by γ-irradiation or bleomycin, downstream events such as checkpoint activation, damage processing and repair occur so quickly that their kinetics appear indistinguishable (Melo and Toczyski, 2002). Here, we exploited the relatively slow response of the yeast cell to a single HO-induced DSB in order to dissect the requirements for Mec1 recruitment, focus formation and checkpoint activation. By analysing this in specific mutants, we were able to determine a hierarchy of interactions that ultimately lead to activation of the DNA-damage checkpoint in response to a single DSB.

Mec1 binds ssDNA in vivo

We showed, by quantitative QAOS, that Mec1 associates with ssDNA at a processed DSB in living cells. This lends credence to both in vitro and in vivo binding studies that have suggested that Mec1-Ddc2 associates with RPA-coated

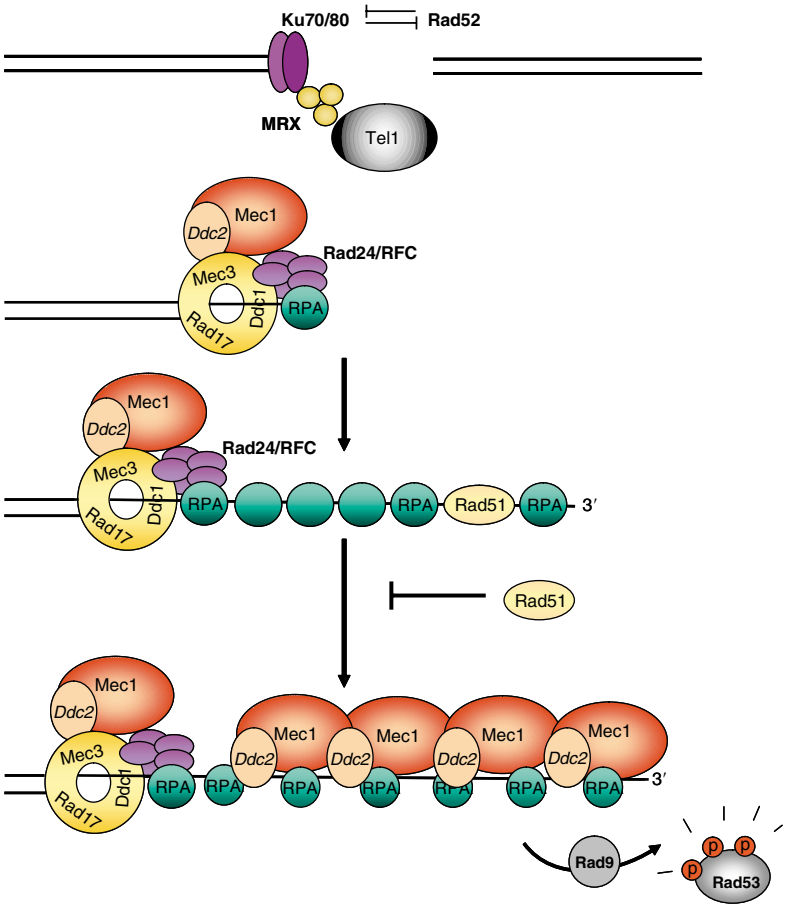

Fig. 7. Steps leading to Mec1-Ddc2 accumulation and checkpoint activation by a DSB. Shown is a summary of the events involved in Mec1-Ddc2 accumulation at a DSB in budding yeast. yKu and the MRX complex bind rapidly and recruit Tel1 (ATM). At this early stage, a low level of Mec1-Ddc2 can also be detected. The resection of the end by Rad24 and the 9-1-1 complex (Rad17, Mec3 and Ddc1) leads to the loading of RPA. The OB-fold domain 1 of RPA recruits Mec1-Ddc2 and this is antagonised by Rad51. Resection and Mec1-Ddc2 recruitment both appear to be aided by Rad24/9-1-1. Sufficient accumulation of Mec1-Ddc2 becomes visible as a 'focus' and the downstream checkpoint activation of Rad53, stimulated by Rad9, occurs.

ssDNA at lesions (Nakada et al., 2004; Nakada et al., 2005; Rouse and Jackson, 2002; Zou and Elledge, 2003). Our genetic analysis revealed a slight increase in Mec1 recruitment in the *yku70* mutant, which correlates with the increase in the rate of processing observed in this mutant (Lee et al., 1998). Conversely, Mec1 recruitment was reduced in the *rad9 rad24* mutant, which accumulated ssDNA much more slowly. These results rule out a requirement for yKu in Mec1 recruitment and show that Rad24 and/or its associated complexes can modulate Mec1 recruitment at a DSB. Because Mec1 has been shown to interact in vitro and in vivo with the ssDNA-binding protein RPA (Nakada et al., 2005; Zou et al., 2003), impaired Mec1 binding near the DSB in the *rad24* mutant could be explained by a drop in RPA-bound ssDNA. However, in the absence of Rad24, an equivalent accumulation of ssDNA did not mediate the same level of Mec1 recruitment, suggesting that Rad24 plays an additional role in these events (Fig. 5B).

Rad24-RFC regulates Mec1 recruitment to DSBs

Rad24 is related to subunits of Replication factor C, with which it forms a complex that loads a PCNA-like complex composed of Rad17-Mec3-Ddc1 (called 9-1-1 in other organisms) at sites of damage. The loading of this complex and Mec1-Ddc2 binding are necessary events for full activation of the Rad53-dependent damage-checkpoint response (Melo et al., 2001). It has been shown in vitro that Rad24 cooperates with RPA to load the Rad17-Mec3-Ddc1 complex at the 5′ junction of partially resected DNA (Majka et al., 2006a; Zou et al., 2003). Indeed, activation of Mec1 in vitro depends on the appropriate loading of the Rad17-Mec3-Ddc1 complex by Rad24 onto DNA (Majka et al., 2006b). In contrast to what was previously published, our kinetics and quantitative ChIP analysis of Mec1 recruitment allowed us to reveal a requirement for Rad24 in the binding of Mec1 to DSBs. This observation is further confirmed by the decrease of focus formation that we observed in the *rad24* mutant. Part of the decrease in Mec1 focus formation that we observed in *rad24* mutants in vivo might reflect the inefficient loading of the Rad17-Mec3-Ddc1 complex.

We examined the nature of Mec1-bound DNA and confirm that a fraction of Mec1 is bound to sites containing both ss and dsDNA (Fig. 4F). Based on in vitro data, Majka et al. have argued that the Rad17-Mec3-Ddc1 complex loads preferentially at 5′ ds-ssDNA junctions in the presence of RPA (Majka et al., 2006b). Thus, the fraction of Mec1 that is associated with ss and dsDNA might reflect a population recruited by Rad24/Rad17-Mec3-Ddc1, either through direct protein-protein interaction or via another unidentified mechanism. Our data are thus consistent with the proposal that Rad24 contributes to Mec1 recruitment not only by promoting ssDNA formation and RPA binding, but also by mediating Mec1-Ddc2 binding at the ds-ssDNA junction. The degree to which Mec1-Ddc2 is able to spread along dsDNA is unknown. However, the Mec1-dependent phosphorylation of histone H2A spreads over 50 kb even in the absence of Tel1 (Shroff et al., 2004), suggesting an ability of Mec1-Ddc2 to diffuse along chromatin.

RPA and Rad24 cooperate to recruit Mec1 to DSB

Even though the association of the Rad17-Mec3-Ddc1 complex with a DSB does not require long ssDNA tracts (Nakada et al., 2004), the loading of Rad24 and Rad17-Mec3-Ddc1 complexes onto DNA templates was shown to be impaired in the presence of *rfa1*-t11 (Majka et al., 2006a). We report here a significant reduction in Mec1 accumulation at the DSB in the *rfa1*-t11 mutant. This reduction is unlikely to stem solely from a reduced level of Rad24 binding, because *rad24* and *rfa1*-t11 phenotypes are clearly distinct. First, we note that the rate of end-resection was compromised in *rad24* mutants, yet resection occurred at wild-type levels in *rfa1*-t11 cells. Second, the *rfa1*-t11 and *rad24* mutants showed distinct phenotypes with respect to Mec1 recruitment and focus

formation. In a *rad24*-null mutant, there were still 8% of the cells with Mec1 foci, whereas, in the *rfa1*-t11 mutant, foci were not detected. Moreover, recruitment of Mec1 was affected at early time points in the *rad9 rad24* mutant, whereas, in *rfa1*-t11 cells, Mec1 levels were reduced primarily at later time points. Consistent with this, it was shown that the *rfa1*-t11 mutant protein loads 4-5 times less Ddc2 onto ssDNA in vitro (Zou et al., 2003), suggesting that Mec1-Ddc2 could be recruited to ssDNA by direct interaction with Rfa1. Taken together, these observations argue that Rad24 and Rfa1 function on distinct pathways to recruit Mec1 to DSBs. Nonetheless, these two pathways might be interdependent, because Rad24 participates in RPA loading by providing ssDNA, and RPA facilitates and orientates Rad24 loading onto the ds-ssDNA junction (see Model, Fig. 7).

Mec1 recruitment is regulated by competition between RPA and Rad51

The notion that Mec1 is recruited to ssDNA through direct contact with Rfa1 is further supported by the fact that Mec1 recruitment and focus formation are influenced in opposite ways by the loss of the ssDNA-binding factors Rad51 and Rfa1. Importantly, neither phenotype correlated strictly with a change in the rate of end-resection (Fig. 4). We observed that Mec1 was more efficiently recruited and formed foci more efficiently in *rad51* mutants, a condition under which more RPA is bound to the ssDSB (Wang and Haber, 2004). If Rad51 binding reduces Mec1 accumulation at a processed DSB, this would provide a means to forestall checkpoint activation when repair by homologous recombination occurs rapidly. Indeed, when donor sequences are present as HMR and HML loci, cleavage at *MAT* by the HO endonuclease does not provoke Mec1-Ddc2 focus formation and cell cycle arrest through checkpoint activation (Pellicioli et al., 2001). This model links end-processing and competition between different ssDNA binding factors to Mec1 focus formation and checkpoint activation.

Mec1 recruitment to the DSB modulates checkpoint activation

The kinetics of Mec1 recruitment to a DSB are independent of downstream checkpoint responses. However, we can correlate high levels of Mec1-Ddc2 accumulation at 2-4 hours after HO induction with the activation of Rad53, suggesting a causal relationship. Our genetic analysis reinforces the correlation between Mec1 focus formation and checkpoint activation: the deletion of *rad24* and the *rfa1*-t11 mutation both impair Mec1 focus formation and lower checkpoint activation, whereas the *rad51* mutation increases both focus formation and checkpoint activation (Figs 3, 5). We suggest that accumulation of a threshold level of Mec1 at a DSB is required for activation of a robust Rad53-mediated checkpoint response. Surprisingly, however, Rad53 itself did not accumulate at the processed DSB. This might reflect its role as an effector kinase, rather than a sensor in the checkpoint-activation process.

Mec1 and/or Ddc2 have also been shown to be recruited to other types of DNA damage in yeast. Given that Mec1 localises to stalled replication forks and uncapped telomeres in the *cdc13-1* mutant, the RPA-coated ssDNA might be a more general recruitment signal for Mec1 (Rouse and Jackson, 2002; Sogo et al., 2002). By contrast, when telomeres are susceptible to resection (i.e. in the *cdc13-1* mutant at non-permissive temperature) or after γ-irradiation, Mec1-Ddc2 recruitment appears to occur independently of Rad24 (Melo et al., 2001; Rouse and Jackson, 2002). Moreover, Mec1-Ddc2 is able to bind at stalled forks in *rfa1*-t11 mutants, even though Rad17-Mec3-Ddc1 binding is affected (Kanoh et al., 2006). These cases argue for lesion-specific variation in the trigger for Mec1-Ddc2 recruitment. Nonetheless, the generation of RPA-coated ssDNA through the action of Mre11 and MRN was recently shown to be required for the recruitment of ATR-ATRIP in mammalian cells (Adams et al., 2006; Jazayeri et al., 2006). Thus, it seems likely that the mechanisms described here for the recruitment of Mec1-Ddc2 to DSBs are conserved from yeast to human.

Materials and Methods

Yeast strains and media

Standard culture conditions at 30°C and media were used. For HO endonuclease induction, strains were grown on rich medium containing 3% glycerol, 2% lactic acid and 0.05% glucose overnight, prior to adding 2% galactose or 2% glucose for the negative control. Yeast strains are in supplementary Table S1. For strain construction, the *MEC1* gene was tagged with 18 Myc epitopes by inserting the *Stu*I-digested plasmid pML191.17 into JKM179 (Lee et al., 1998; Paciotti et al., 2000). The *rfa1*-t11 *Myc-MEC1* strain was similarly constructed by insertion into YSL31 (Lee et al., 1998). The *Myc-mec1-kd1* tagging was obtained by transformation of the *Myc-MEC1 sml1* deletion strain (GA1817) with the *Xho*I-digested plasmid pML228.1 (Paciotti et al., 2001), followed by excision of the *URA3* marker. A tandem array of 256 *lac* operators was integrated 4.4 kb upstream of the HO recognition site within *MATalpha* in JKM179, which was modified to express a non-tetramerising *lac* repressor-GFP fusion under the *HIS3* promoter (Heun et al., 2001; Straight et al., 1996). Western blots were performed to confirm proper tagging. The following complete null alleles were created in JKM179 using PCR-based gene disruption techniques and primers located within 100 bp of the beginning and end of each gene (Longtine et al., 1998): *yku70*::*URA3*, *sml1*::*kanMX6*, *mec1*::*TRP1*, *rad9*::*TRP1*, *rad53*::*kanMX6*, *sml1*::*TRP1*, *ddc2*::*TRP1*, *arp8*::*kanMX4* and *swr1*::*kanMX4*. The *rad24*::*kanMX* deletion was mediated by transforming with a mixture of pKAS1Rad24 and pANS2Rad24 digested with *Not*I (Fairhead et al., 1996). Disruption of *RAD51* was done using the plasmid pTZ51Δ (Aboussekhra et al., 1992).

Immunofluorescence

For IF assays, exponentially growing cells were subjected to spheroplasting in YPD containing 1.1 M sorbitol prior to formaldehyde fixation and staining as described (Gotta et al., 1999). Commercial antibodies have all been previously described (Martin et al., 1999). Image acquisition was performed taking a single 0.4 μm mid-cell confocal section on the Zeiss LSM510 confocal microscope. Mec1 signals were not normalised but represent the original scanned intensity. Foci were scored on at least 100 cells. Ddc2-YFP foci were counted on maximal projections of 21-image *z*-stacks (200-nm step size) captured on a Metamorph-driven Nikon TE2000 microscope. Foci were scored on two independent experiments and at least 200 cells.

Chromatin immunoprecipitation

ChIP and multiplex PCR was performed as described (Martin et al., 1999), except that immunoprecipitation was performed for 2 hours. PCR products were resolved by electrophoresis (see supplementary material Fig. S1) and quantified with a Biorad Fluo-imager. Accuracy of the multiplex method and enrichment for Myc-Mec1 at *MAT* in wild-type, *rfa1*-t11 and *rad51* strains were verified and determined by real-time PCR on the Perkin-Elmer ABI Prism 7700 Sequence Detector System, using appropriate primers and probe sites (primer sequences available upon request), respectively. Fold enrichment was calculated as described (van Attikum et al., 2007; Martin et al., 1999).

Quantitative analysis of ssDNA (QAOS)

ssDNA was measured as described by quantitative real-time PCR analysis (Booth et al., 2001), except that we calculated ssDNA percentages based on total denatured HO1 signal for each time point and sample, because the global amount of HO1 sequence decreases over time. Primer sequences are available upon request. To assess the nature of the DNA immunoprecipitated, DNA from input (total), IP or non-sonicated DNA was treated for 3 hours at 37°C with the 5′-to-3′ exonuclease RecJ (New England Biolabs) prior to ssDNA measurement by QAOS.

In situ autophosphorylation assay (ISA)

Extract preparation, western blot procedure and in situ autophosphorylation assay were performed as described (Pellicioli et al., 1999). Equal loading of the gels was assessed by staining with the anti-tubulin antibody TAT1.

This work was funded by the Swiss Cancer League, Swiss National Science Foundation and the Novartis Research Foundation to S.M.G., and fellowships from EMBO to K.D. and H.v.A., and from HFSP to H.v.A. We thank J. Haber, S. Marcand and M. P. Longhese for generously providing strains and plasmids, and S. Marcand for critically reading the manuscript. Work was performed in part at the Department of Molecular Biology, University of Geneva, Switzerland, and at the UMR218, Institut Curie, Paris, France.

References

Aboussekhra, A., Chanet, R., Adjiri, A. and Fabre, F. (1992). Semidominant suppressors of Srs2 helicase mutations of Saccharomyces cerevisiae map in the RAD51 gene, whose sequence predicts a protein with similarities to procaryotic RecA proteins. *Molec. Cell. Biol.* **12**, 3224-3234.

Adams, K. E., Medhurst, A. L., Dart, D. A. and Lakin, N. D. (2006). Recruitment of ATR to sites of ionising radiation-induced DNA damage requires ATM and components of the MRN protein complex. *Oncogene* **25**, 3894-3904.

Aylon, Y. and Kupiec, M. (2003). The checkpoint protein Rad24 of S. cerevisiae is involved in processing double-strand break ends and in recombination partner choice. *Mol. Cell. Biol.* **23**, 6585-6596.

Booth, C., Griffith, E., Brady, G. and Lydall, D. (2001). Quantitative amplification of single-stranded DNA (QAOS) demonstrates that cdc13-1 mutants generate ssDNA in a telomere to centromere direction. *Nucleic Acids Res.* **29**, 4414-4422.

Fairhead, C., Llorente, B., Denis, F., Soler, M. and Dujon, B. (1996). New vectors for combinatorial deletions in yeast chromosomes and for gap-repair cloning using 'split-marker' recombination. *Yeast* **12**, 1439-1457.

Falck, J., Coates, J. and Jackson, S. P. (2005). Conserved modes of recruitment of ATM, ATR and DNA-PKcs to sites of DNA damage. *Nature* **434**, 605-611.

Frank-Vaillant, M. and Marcand, S. (2002). Transient stability of DNA ends allows nonhomologous end joining to precede homologous recombination. *Mol. Cell* **10**, 1189-1199.

Gotta, M., Laroche, T. and Gasser, S. M. (1999). Analysis of nuclear organization in Saccharomyces cerevisiae. *Meth. Enzymol.* **304**, 663-672.

Heun, P., Laroche, T., Raghuraman, M. K. and Gasser, S. M. (2001). The positioning and dynamics of origins of replication in the budding yeast nucleus. *J. Cell Biol.* **152**, 385-400.

Jazayeri, A., Falck, J., Lukas, C., Bartek, J., Smith, G. C., Lukas, J. and Jackson, S. P. (2006). ATM- and cell cycle-dependent regulation of ATR in response to DNA double-strand breaks. *Nat. Cell Biol.* **8**, 37-45.

Jeggo, P. A., Carr, A. M. and Lehmann, A. R. (1998). Splitting the ATM: distinct repair and checkpoint defects in ataxia-telangiectasia. *Trends Genet.* **14**, 312-316.

Kanoh, Y., Tamai, K. and Shirahige, K. (2006). Different requirements for the association of ATR-ATRIP and 9-1-1 to the stalled replication forks. *Gene* **377**, 88-95.

Kondo, T., Wakayama, T., Naiki, T., Matsumoto, K. and Sugimoto, K. (2001). Recruitment of Mec1 and Ddc1 checkpoint proteins to double-strand breaks through distinct mechanisms. *Science* **294**, 867-870.

Lee, S. E., Moore, J. K., Holmes, A., Umezu, K., Kolodner, R. D. and Haber, J. E. (1998). Saccharomyces Ku70, mre11/rad50 and RPA proteins regulate adaptation to G2/M arrest after DNA damage. *Cell* **94**, 399-409.

Lisby, M., Barlow, J. H., Burgess, R. C. and Rothstein, R. (2004). Choreography of the DNA damage response: spatiotemporal relationships among checkpoint and repair proteins. *Cell* **118**, 699-713.

Longtine, M. S., McKenzie, A., 3rd, Demarini, D. J., Shah, N. G., Wach, A., Brachat, A., Philippsen, P. and Pringle, J. R. (1998). Additional modules for versatile and economical PCR-based gene deletion and modification in S. cerevisiae. *Yeast* **14**, 953-961.

Lovett, S. T. and Kolodner, R. D. (1989). Identification and purification of a ssDNA specific exonuclease encoded by the RecJ gene of E. coli. *Proc. Natl. Acad. Sci. USA* **86**, 2627-2631.

Lydall, D. and Weinert, T. (1995). Yeast checkpoint genes in DNA damage processing: implications for repair and arrest. *Science* **270**, 1488-1491.

Majka, J., Binz, S. K., Wold, M. S. and Burgers, P. M. (2006a). Replication protein A directs loading of the DNA damage checkpoint clamp to 5′-DNA junctions. *J. Biol. Chem.* **281**, 27855-27861.

Majka, J., Niedziela-Majka, A. and Burgers, P. M. (2006b). The checkpoint clamp activates Mec1 kinase during initiation of the DNA damage checkpoint. *Mol. Cell* **24**, 891-901.

Mantiero, D., Clerici, M., Lucchini, G. and Longhese, M. P. (2007). Dual role for S. cerevisiae Tel1 in the checkpoint response to double-strand breaks. *EMBO Rep.* **8**, 380-387.

Maringele, L. and Lydall, D. (2002). EXO1-dependent single-stranded DNA at telomeres activates subsets of DNA damage and spindle checkpoint pathways in budding yeast yku70Delta mutants. *Genes Dev.* **16**, 1919-1933.

Martin, S. G., Laroche, T., Suka, N., Grunstein, M. and Gasser, S. M. (1999). Relocalization of telomeric Ku and SIR proteins in response to DNA strand breaks in yeast. *Cell* **97**, 621-633.

Melo, J. and Toczyski, D. (2002). A unified view of the DNA-damage checkpoint. *Curr. Opin. Cell Biol.* **14**, 237-245.

Melo, J. A., Cohen, J. and Toczyski, D. P. (2001). Two checkpoint complexes are independently recruited to sites of DNA damage in vivo. *Genes Dev.* **15**, 2809-2821.

Nakada, D., Hirano, Y. and Sugimoto, K. (2004). Requirement of the Mre11 complex and exonuclease 1 for activation of the Mec1 signaling pathway. *Mol. Cell. Biol.* **24**, 10016-10025.

Nakada, D., Hirano, Y., Tanaka, Y. and Sugimoto, K. (2005). Role of the C terminus of Mec1 checkpoint kinase in its localization to sites of DNA damage. *Mol. Biol. Cell* **16**, 5227-5235.

Nyberg, K. A., Michelson, R. J., Putnam, C. W. and Weinert, T. A. (2002). Toward maintaining the genome: DNA damage and replication checkpoints. *Annu. Rev. Genet.* **36**, 617-656.

Paciotti, V., Clerici, M., Lucchini, G. and Longhese, M. P. (2000). The checkpoint protein Ddc2, functionally related to S. pombe Rad26, interacts with Mec1 and is regulated by Mec1-dependent phosphorylation in budding yeast. *Genes Dev.* **14**, 2046-2059.

Paciotti, V., Clerici, M., Scotti, M., Lucchini, G. and Longhese, M. P. (2001). Characterization of mec1 kinase-deficient mutants and of new hypomorphic mec1 alleles impairing subsets of the DNA damage response pathway. *Mol. Cell. Biol.* **21**, 3913-3925.

Pellicioli, A., Lucca, C., Liberi, G., Marini, F., Lopes, M., Plevani, P., Romano, A., Di Fiore, P. P. and Foiani, M. (1999). Activation of Rad53 kinase in response to DNA damage and its effect in modulating phosphorylation of the lagging strand DNA polymerase. *EMBO J.* **18**, 6561-6572.

Pellicioli, A., Lee, S. E., Lucca, C., Foiani, M. and Haber, J. (2001). Regulation of Saccharomyces Rad53 checkpoint kinase during adaptation from DNA damage-induced G2/M arrest. *Mol. Cell* **7**, 293-300.

Rouse, J. and Jackson, S. P. (2000). LCD1: an essential gene involved in checkpoint control and regulation of the MEC1 signalling pathway in S. cerevisiae. *EMBO J.* **19**, 5801-5812.

Rouse, J. and Jackson, S. P. (2002). Lcd1p recruits Mec1p to DNA lesions in vitro and in vivo. *Mol. Cell* **9**, 857-869.

Sanchez, Y., Desany, B. A., Jones, W. J., Liu, Q., Wang, B. and Elledge, S. J. (1996). Regulation of RAD53 by the ATM-like kinases MEC1 and TEL1 in yeast cell cycle checkpoint pathways. *Science* **271**, 357-360.

Shiloh, Y. (2003). ATM and related protein kinases: safeguarding genome integrity. *Nat. Rev. Cancer* **3**, 155-168.

Shroff, R., Arbel-Eden, A., Pilch, D., Ira, G., Bonner, W. M., Petrini, J. H., Haber, J. E. and Lichten, M. (2004). Distribution and dynamics of chromatin modification induced by a defined DNA double-strand break. *Curr. Biol.* **19**, 1702-1711.

Sogo, J. M., Lopes, M. and Foiani, M. (2002). Fork reversal and ssDNA accumulation at stalled replication forks owing to checkpoint defects. *Science* **297**, 599-602.

Straight, A. F., Belmont, A. S., Robinett, C. C. and Murray, A. W. (1996). GFP tagging of budding yeast chromosomes reveals that protein-protein interactions can mediate sister chromatid cohesion. *Curr. Biology* **6**, 1599-1608.

Sung, P. (1997). Yeast Rad55 and Rad57 proteins form a heterodimer that functions with replication protein A to promote DNA strand exchange by Rad51 recombinase. *Genes Dev.* **11**, 1111-1121.

Umezu, K., Sugawara, N., Chen, C., Haber, J. E. and Kolodner, R. D. (1998). Genetic analysis of yeast RPA1 reveals its multiple functions in DNA metabolism. *Genetics* **148**, 989-1005.

van Attikum, H., Fritsch, O. and Gasser, S. M. (2007). Distinct roles for SWR1 and INO80 chromatin remodeling complexes at chromosomal double-strand breaks. *EMBO J.* **26**, 4113-4125.

Wang, X. and Haber, J. E. (2004). Role of Saccharomyces single-stranded DNA-binding protein RPA in the strand invasion step of double-strand break repair. *PLoS Biol.* **2**, E21.

Wright, J. A., Keegan, K. S., Herendeen, D. R., Bentley, N. J., Carr, A. M., Hoekstra, M. F. and Concannon, P. (1998). Protein kinase mutants of human ATR increase sensitivity to UV and ionizing radiation and abrogate cell cycle checkpoint control. *Proc. Natl. Acad. Sci. USA* **95**, 7445-7450.

Zhao, X., Muller, E. G. and Rothstein, R. (1998). A suppressor of two essential checkpoint genes identifies a novel protein negatively affecting dNTP pools. *Mol. Cell* **2**, 329-340.

Zou, L. and Elledge, S. J. (2003). Sensing DNA damage through ATRIP recognition of RPA-ssDNA complexes. *Science* **300**, 1542-1548.

Zou, L., Liu, D. and Elledge, S. J. (2003). Replication protein A-mediated recruitment and activation of Rad17 complexes. *Proc. Natl. Acad. Sci. USA* **100**, 13827-13832.